DOI 10.31489/2021Ph3/35-44
UDC 533.9.082

A.A. Mutalip[1,2*], Y.A. Ussenov[1,2], A.K. Akildinova[1,2],
M.K. Dosbolayev[3], M.T. Gabdullin[1,4], T.S.Ramazanov[3]

[1]*NNLOT, Faculty of Physics and Technology, Al-Farabi Kazakh National University, Almaty, Kazakhstan;*
[2]*Institute of Applied Science and Information Technologies, Almaty, Kazakhstan;*
[3]*IETP, Faculty of Physics and Technology, Al-Farabi Kazakh National University, Almaty, Kazakhstan;*
[4]*Kazakhstan-British Technical University, Almaty, Kazakhstan*
([*]*E-mail: mutalip.abdurashid@gmail.com)*

Determination of the reduced electric field in surface dielectric barrier discharge plasmas

In this paper the experimental determination of the reduced electric field (E/n) in plasma of dielectric coplanar surface barrier discharge (DCSBD) at atmospheric pressure was demonstrated. The plasma characteristics and the experimental setup properties were described, and the optical emission spectrum of the plasma was also measured. The results of optical emission spectroscopy showed the presence of nitrogen molecular bands in the emission spectrum of DCSBD. In particular, the second positive and the first negative systems, as well as low intensity OH and NO lines were identified. The main transport properties of electrons, such as mobility, mean average energy, and diffusion coefficients were calculated using the BOLSIG+ open source software. The dependence of the ratio of intensities of the nitrogen spectral lines on the reduced electric field, the dependence of the E/n on plasma power, and the dependence of the electron energy distribution function (EEDF) on E/n were obtained. An algorithm in the form of a block diagram for determining the reduced electric field by the BOLSIG + program and experimentally measured spectral line intensities are presented. The utilized method are quite simple, accessible and versatile.

Keywords: plasma, dielectric barrier discharge, spectroscopy, reduced electric field, lines intensity, nitrogen spectrum, Boltzmann equation.

Introduction

Dielectric barrier discharge (DBD) is a discharge ignited between electrodes, one or both of which are covered with a dielectric [1, 2]. The DBD can generate high-density atmospheric pressure plasma jets using an air flow as a source gas [3]. At the same time, the generation of DBD does not require large vacuum installations, which favorably distinguishes its operation in comparison with other types of discharges [4]. Another distinctive feature of the dielectric barrier discharge is the ability to generate low-temperature, “cold” plasma at atmospheric pressure, which is a key point in the processing of crops, biological samples, and various polymeric and heat sensitive materials. Also, atmospheric pressure plasma (APP), obtained on the basis of a dielectric barrier discharge, is widely used in plasma medicine, water disinfection, nanotechnology and thin film coating [5, 6].

There are two types of dielectric barrier discharge: volume dielectric barrier discharge and surface dielectric barrier discharge. A bulk DBD consists of two parallel electrodes covered with a dielectric layer, or two electrodes located on a dielectric plate. Plasma is generated in the volume of the gap between the electrodes. The configuration of the surface dielectric barrier discharge is as follows: one electrode is located on the surface of the dielectric plate, the other electrode is embedded on the other side of this plate and the discharge is ignited directly on the surface of the dielectric [7]. There is also a surface coplanar dielectric barrier discharge, which occupies an intermediate position between volume and surface discharges. The difference between this discharge is that both electrodes are built in into the dielectric, and the discharge is ignited on the surface of the dielectric.

The wide range of applications of atmospheric pressure plasmas requires a detailed study of the optical properties. The electric field plays a key role in the motion and spatial distribution of charged particles in low-temperature plasmas. The advantage of optical diagnostic methods is that they are non-contact and do not affect the object under the test. Methods based on optical radiation or absorption are characterized by relatively simple measurement equipments.

Several spectroscopic methods can be used to determine the values of the electric field. One of the optical methods is Thomson scattering. However, in such case the scattered laser signal is very weak and several orders of magnitude lower than the incident laser beam, and therefore requires an accurate and expensive installation to evaluate it. Also, there are special requirements for the laser: the laser power must be high

enough to obtain an intense scattered signal, and at the same time laser radiation should not introduce perturbations on the diagnosed plasma itself [8].

The Stark shifting is also used to measure the electric field of atmospheric pressure plasmas. Stark polarization spectroscopy uses the Stark effect, which affects the emission spectra depending on the local electric field. Electric fields cause a splitting of energy levels, and a shift of these levels, depending on the electric field. In general, the Stark shift is widely used for dense plasma with electron density above 10^{16} cm^{-3}, and for these plasma conditions, the theoretical data that can be taken for evaluation are well studied. However, this method requires a monochromator with very high resolution, which is usually not easily available [9].

The method of fluorescence spectroscopy includes exposure of the object under study and collection of scattered radiation. Next, a spectrum is generated with different intensities in a given wavelength range. The disadvantage of this method is the necessity to use additional CCD (charge-coupled device) cameras, for visualization of laser-induced fluorescence, which complicates the measurement process [10].

This article demonstrates the determination of the reduced electric field (E/n) of a coplanar surface barrier discharge by measuring optical emission spectroscopy and solving the Boltzmann equation [11]. The described method is quite simple, accessible and versatile.

Experimental setup

The experiments were carried out on an RPS400 setup. The RPS400 is an atmospheric pressure plasma generator which provides an uniform plasma area of approximately 8 cm x 20 cm. The RPS400 system uses a diffuse coplanar surface barrier discharge cell to generate plasma at ambient air, which enables the processing of plastics, metal, wood and glass based products. A schematic diagram of the DCSBD setup is shown in Figure 1 [12]. The conductive electrodes are parallel to each other and embedded in a ceramic dielectric. Plasma is formed on the ceramic surface over an area of 80 mm * 200 mm and reaches a height of about 0.3 mm. The electrodes are made of silver with width of 1.8 mm, thickness of 0.1 mm, length of 230 mm and are located at a distance of 1 mm from each other. The thickness of the ceramic layer between the electrodes and the plasma is 0.4 mm. The discharge was activated by a sinusoidal high voltage (17 kHz, approximately 3 kV peak-to-peak) supplied with an HV plasma power supply. The power of the supplied discharge can be manually adjusted from 80 W to 400 W.

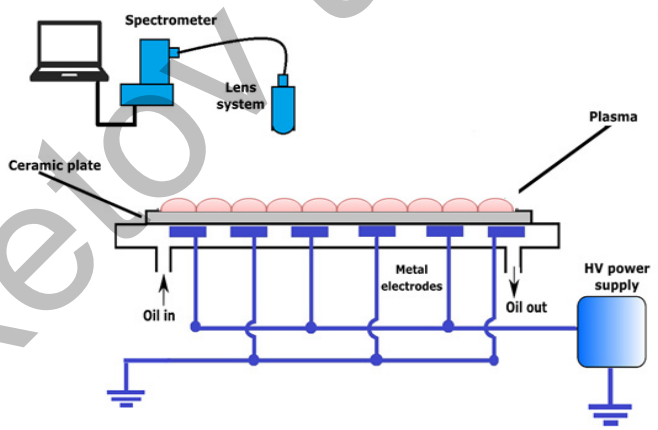

Figure 1. The schematic diagram of electrodes and optical measurement system of DCSBD

Method for determining the reduced electric field

To study the chemical composition and kinetic reactions of the discharge the optical properties of the DCSBD were studied. To achieve this goal the SolarSystems optical emission spectrometer was used. The spectrometer consists of an optical lens system that records a signal collected in a single unit, an optical fiber and the spectrometer itself. Signal registration is performed by a linear Toshiba TDC1304CCD detector. A personal computer was used to digitize and process the signal.

The ratio of the intensities of the spectral lines of nitrogen can be represented in the form of equation (1) [13]. The left side of the equation is the ratio of the intensities of the nitrogen lines, is found experimentally through the obtained spectrum, and the right side, in particular the reaction rate constant (k), is found numerically through the BOLSIG + program [14]. The rest of the values are constant for certain experimental conditions (Table 1):

$$R = \frac{I_B\left(\frac{E}{n}\right)}{I_C\left(\frac{E}{n}\right)} = \frac{k_B\left(\frac{E}{n}\right)\tau_0^C T_B \tau_{air}^B}{k_C\left(\frac{E}{n}\right)\tau_0^B T_C \tau_{air}^C}, \quad (1)$$

where R is the intensity ratio of the nitrogen lines, I is the intensity of the certain line, k is the reaction rate constant, τ_0 is the lifetime of excited or ionized states of nitrogen molecules, T is a parameter that depends on the sensitivity of the photo detector, τ_{air} is the lifetime in air, indices B and C indicate the following reactions (ionization and excitation) of the nitrogen molecule [15]:

$$N_2^+\left(B^2\sum_u^+, \vartheta = 0 \rightarrow X^2\sum_g^+, \vartheta = 0\right), \text{ 391,4 nm},$$
$$N_2\left(C^3\Pi_u, \vartheta = 0 \rightarrow B^3\Pi_g, \vartheta = 0\right), \text{ 337,1 nm}.$$

Table 1

Lifetimes of radiative and of excitation states of some excited states of a nitrogen molecule and ion

Reaction of a nitrogen molecule	*Radiation lifetime* τ_0 *(ns)*	*lifetime of excitation states* τ_{air} *(ns)*
$\left(C^3\Pi_u, \vartheta = 0 \rightarrow B^3\Pi_g, \vartheta = 0\right)$	40	0,62
$\left(B^2\sum_u^+, \vartheta = 0 \rightarrow X^2\sum_g^+, \vartheta = 0\right)$	60	0,134

From the obtained spectrum we could find the ratio of the intensities of the first negative system of the nitrogen molecule $N_2^+\left(B^2\sum_u^+, \vartheta = 0 \rightarrow X^2\sum_g^+, \vartheta = 0\right)$ to the second positive system of the nitrogen molecule $N_2\left(C^3\Pi_u, \vartheta = 0 \rightarrow B^3\Pi_g, \vartheta = 0\right)$, which appear at wavelengths of 391.4 and 337.1 nm, respectively.

At the same time, in the BOLSIG + program we can calculate the reaction rate constant, choosing different values of E/n and appropriate database for cross sections. BOLSIG+ is a free and user-friendly computer program for the numerical solution of the Boltzmann equation for electrons in weakly ionized gases in uniform electric fields, conditions which occur in swarm experiments and in various types of gas discharges and collisional low-temperature plasmas. The principle of the program and the formulas used are described in detail by the authors of this program [11].

When the experimental data coincide with the numerical result (BOLSIG +), we extract the electron energy distribution function (EEDF), which is the main quantity for studying kinetic processes in plasma and other transport properties for their further use in calculations and numerical simulations. If the results do not coincide, we return to the selection of E/n in the BOLSIG + program until they coincide with our experimental results. This algorithm is graphically displayed in Figure 2.

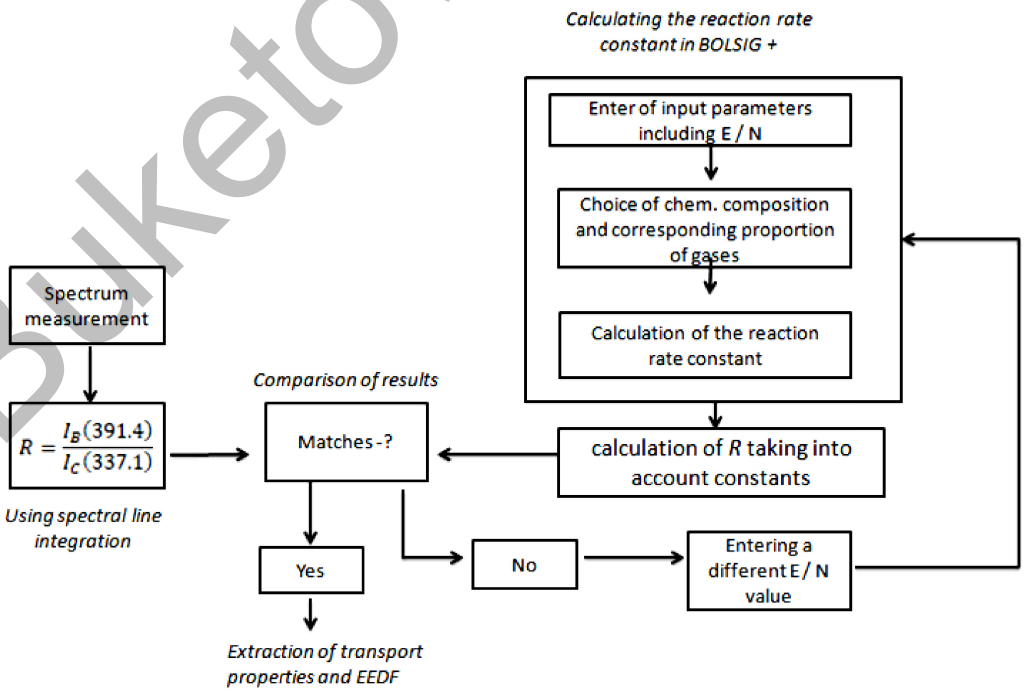

Figure 2. Algorithm for determining the reduced electric field by calculating transport properties in the BOLSIG + program and experimental measurement of the intensities of nitrogen spectral lines

Results and discussion

The experiments were carried out in the plasma power range from 200 W to 400 W with a step of 50 W. It can be seen from the results of the experiment that with an increase in power the surface of the DCSBD discharge cell is gradually filled with multiple microdischarge channels (Fig. 3). Complete filling of the surface is observed at a power of 220 W. At a power of 400 W the surface of the discharge cell is uniformly and closely filled with dense plasma. Below discharge cell surface images are shown at 220 W applied power (the surface is completely filled with micro-discharges) and at a power of 400 W (maximum power) (Fig. 3).

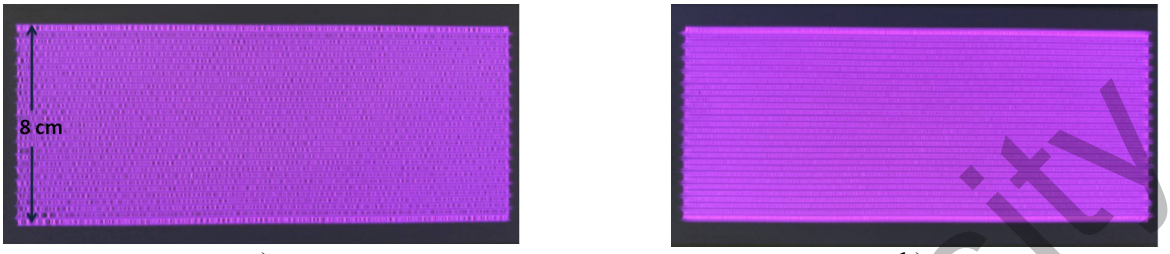

a) b)

Figure 3. Images of the surface of the discharge cell at powers of 220 W (a) and 400 W (b)

Using optical emission spectroscopy, the chemical composition of the DCSBD was determined. Molecular nitrogen bands, namely the second positive (N_2 (C-B)) and the first negative (N_2 + (B-X)) systems were observed in the emission spectrum. In Figure 4 the observed peaks from 300 nm to 470 nm are composed of OH (308 nm) radicals, N_2 (337 nm and 357 nm) and N_2^+ (380 nm, 390 nm, 427 nm and 470 nm). Due to the large number of nitrogen molecules in the atmosphere, nitrogen bands are naturally dominant. OH radicals are also visible due to the presence of water vapor in the air [16]. The line intensities of other radicals and chemically active molecules, such as NO, which are common for air plasma under room conditions, were negligibly low due to the low density and effective collisional quenching of the corresponding excited states.

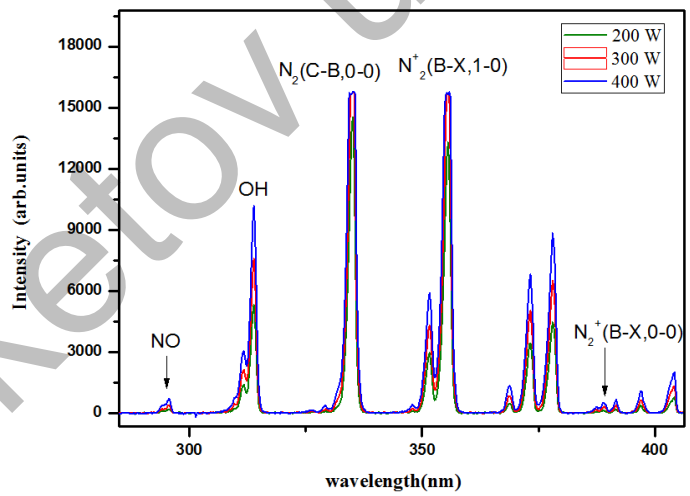

Figure 4. DCSBD spectrum different applied powers

The values $T_B(391{,}4\ \text{nm})$ and $T_C(337{,}1\ \text{nm})$ show the sensitivity of the photodetector at the respective wavelengths. Information on the sensitivity of the photodetector is indicated in the technical documentation. In the technical documentation of our Toshiba TDC1304 optical device the wavelength starts from 400 nm, but we are interested in the wavelength from 300 to 400 nm, namely 337.1 nm and 391.4 nm, where the rotational structures of the nitrogen molecule are recorded. To find the sensitivity of the wavelengths of interest to us, we extrapolated the graphical data (Fig. 5). As a result, the sensitivity ratio of the photodetector at these wavelengths was Tb/Tc = 1.19.

To calculate the total intensity of the nitrogen spectral lines, the molecular spectrum was integrated over the wavelength taking into account the rotational structure of the molecule. After calculating the total intensi-

ty of the lines of interest to us, their ratio was calculated for further comparison with the results obtained by solving the Boltzmann equation.

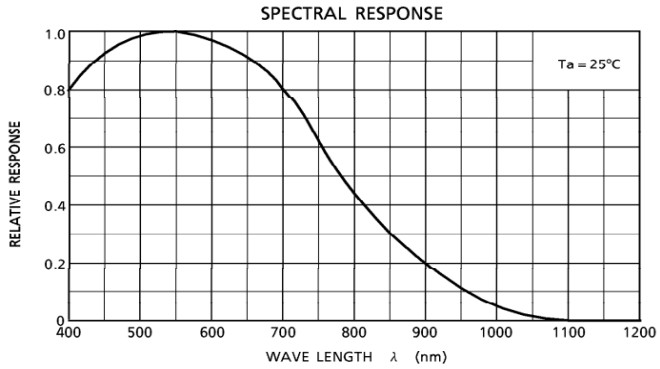

(a)

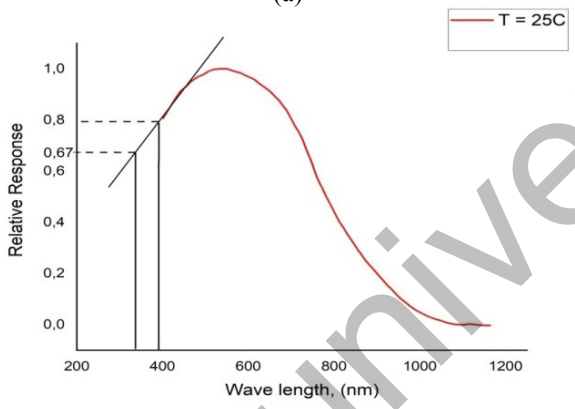

(б)

Figure 5. (a) the sensitivity of the photodetector from 400 to 1200 nm, (b) estimation of the sensitivity in the range of 300–400 nm using the extrapolation of the graph

As mentioned above, the BOLSIG + program was used to solve the Boltzmann equation for electrons. The input parameters are the E/n value, the composition of the plasma-forming gas in a percentage, the degree of ionization, the gas temperature, and the overall density of particles. As a result, the solution of the equation gives transport properties, including the reaction rate constants k, which was subsequently used to numerically calculate the ratio of spectral lines. The rate constants for different values of E/n are shown in Table 2. The results of determining the ratios of spectral lines and their dependence on the values of the reduced electric field are shown in Figure 6. Figure 6 shows that the dependence in the range from 400 to 600 Td is linear. This graph can be used as a gradient-level curve and is convenient in that it allows to quickly and visually evaluate the reduced electric field, comparing it with the obtained experimental ratios of spectral lines.

Table 2

Reaction rate constants for different values of reduced electric field

Reduced electric field E/n (Td)	Reaction rate constants(m^3/s)	
	$N_2(C^3\Pi_u, \vartheta = 0 \rightarrow B^3\Pi_g, \vartheta = 0)$ 11 eV (λ= 337.1 nm)	$N_2^+(B^2\sum_u^+, \vartheta = 0 \rightarrow X^2\sum_g^+, \vartheta = 0)$ 18,7 eV(λ= 391,4nm)
420	0.2032E-14	0.9336E-16
430	0.2085E-14	0.1014E-15
480	0.2330E-14	0.1465E-15
520	0.2503E-14	0.1886E-15
560	0.2658E-14	0.2658E-14

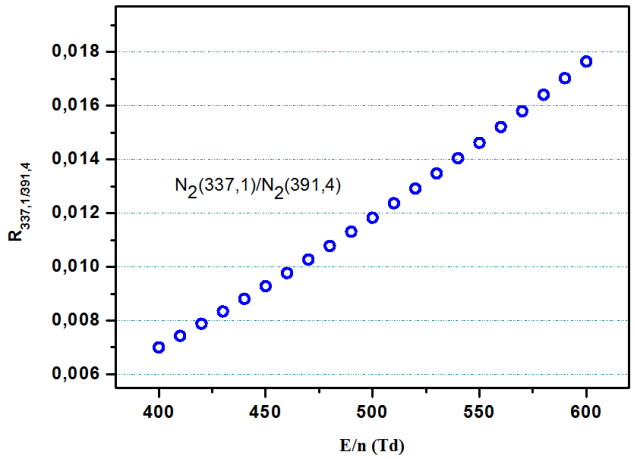

Figure 6. Dependence of the intensity ratio of the spectral lines $N_2^+(391,4)$ and $N_2(337,1)$ on the reduced electric field (E/n)

Further, the above procedure was repeated for different E/n. Figure 7 demonstrates the dependence of the reduced electric field on the discharge power. It is expected that an increase in power leads to an increase in E/n as an increase in power is accompanied by an increase in high-voltage applied to the electrodes of the discharge cell. The obtained values of E/n for air plasma in a surface barrier discharge are in agreement with the results of other related works [17,18] where the investigated plasma and discharge geometry, conditions are quite similar.

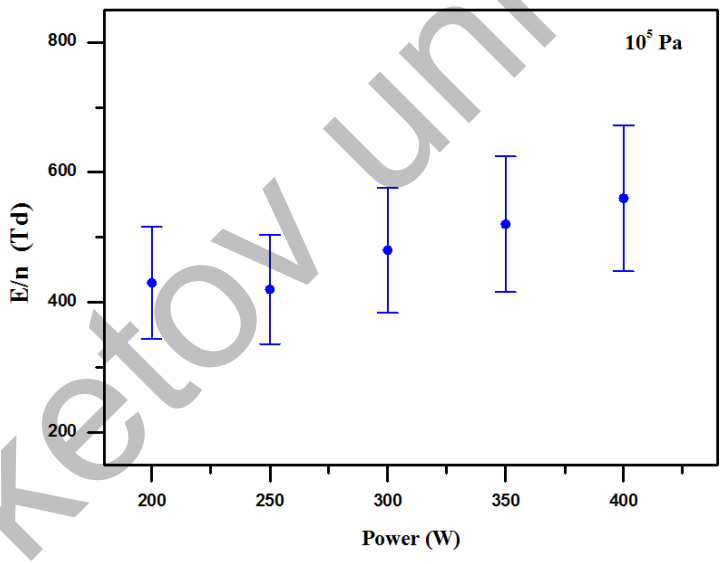

Figure 7. Dependence of the reduced electric field on the discharge power

EEDF is important for studying the various properties of the plasma, since it is necessary for characterization of kinetic processes with the participation of electrons [19]. The EEDF obtained for different values of the reduced electric field shows an increase in the energy and also in the number of fast electrons at the tail of the distribution (Fig. 8). At the same time, the number of low-energy electrons decreases slightly. The increase in the electron energy can be explained by the fact that the increase in E/n makes an additional contribution to the kinetic energy of the electrons, since the electrons mainly gain the energy due to the electric field, accelerating by the Coulomb forces in the gaseous medium. In our case, an increase in E/n means a direct increase in the electric field, since the pressure of the plasma-forming gas remains constant at room conditions. A slight decrease in the number of low-energy electrons is due to the fact that their energy also increases and they contribute to the number of high energy electrons on the tail of the EEDF.

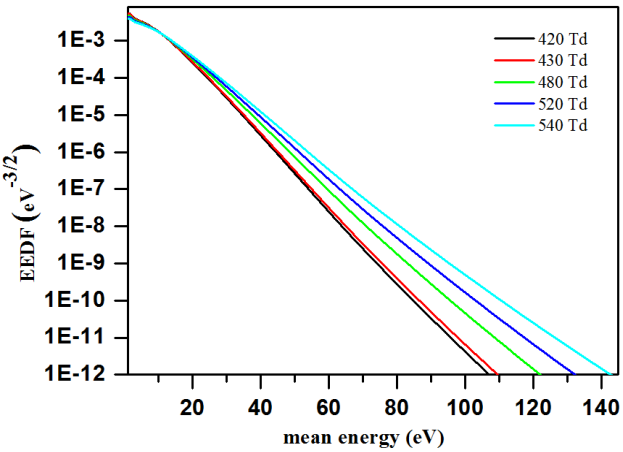

Figure 8. The electron energy distribution function at different values of the reduced electric field

In addition to the EEDF, solving the Boltzmann equation using the BOLSIG + program makes it possible to determine the transport properties of electrons, such as average energy, mobility, diffusion coefficient, and Townsend coefficient, the results of which are shown in Table 3.

Table 3

Transport coefficients for different values of the power

Power (W)	Mean energy (eV)	Mobility*N ((m*V*s)$^{-1}$)	Diffusion coefficient ((m*s)$^{-1}$)	Townsend coefficient α (m^{-1})
200	8.962	0.8318E+24	0.5339E+25	0.4318E-20
250	9.098	0.8264E+24	0.8264E+241	0.4535E-20
300	9.643	0.8067E+24	0.5562E+25	0.5427E-20
350	10.18	0.7888E+24	0.5732E+25	0.6345E-20
400	10.71	0.7722E+24	0.5894E+25	0.7279E-20

The quantitative values of these parameters allows to correctly model and calculate various kinetic properties of a gas-discharge plasma at atmospheric pressure by different numerical simulation methods.

Conclusion

A method for the determination of the reduced electric field (E/n) of diffuse surface dielectric barrier discharge plasma by emission spectra was demonstrated. The method is based on the experimental measurement of the intensity ratio of nitrogen spectral lines and the solution of the Boltzmann equation. The experiments were carried out at different applied powers from 200 W to 400 W with a step of 50 W. The dependence of the line intensity ratio on E/n was obtained, and the main transport properties of electrons and EEDF, which are necessary for numerical simulation of plasma properties, were calculated. The dependence of E/n on the applied discharge power was plotted. The obtained experimental data might be useful for the study of kinetic processes of DCSBD plasma.

Acknowledgment: This work was supported by a grant AP08052056 from the Science Committee of the Ministry of Education and Science of the Republic of Kazakhstan.

References

1 Brandenburg R. Dielectric barrier discharges: Progress on plasma sources and on the understanding of regimes and single filaments / R.Brandenburg // Plasma Sources Sci. Technol. — 2017. — Vol. 26(5). — P. 3001. DOI: 10.1088/1361–6595/AA6426

2 Akishev Y.S. Role of the volume and surface breakdown in a formation of microdischarges in a steady-state DBD / Y.S. Akishev, G. Aponin, A. Balakirev, M. Grushin, V. Karalnik, N. Trushkin // Eur. Phys. J. D. — 2011. –Vol. 61(2). — P. 421–429. DOI: 10.1140/epjd/e2010–10219–7

3 Usenov E.A. The Memory Effect of Microdischarges in the Barrier Discharge in Airflow / E.A. Usenov, Yu.S. Akishev, A.V. Petryakov, T.S. Ramazanov, M.T. Gabdullin & A. Ashirbek // Plasma Phys. Reports. — 2020. — Vol. 46(4). — P. 459–464. DOI: 10.1134/S1063780X20040145

4 Penkov O. A review of recent applications of atmospheric pressure plasma jets for materials processing / O. Penkov, M. Khadem, Won Suk Lim, Dae-Eun Kim // Journal of Coatings Technology and Research. — 2015. — Vol. 12(1). — P. 225–235. DOI: 10.1007/s11998–014–9638-z

5 Ussenov Y.A. Dust Particle Synthesis by the Combined Plasma Source at Atmospheric Pressure / Y.A. Ussenov, A.S. Pazyl, M.K. Dosbolayev, M.T. Gabdullin, T.T. Daniyarov, T.S. Ramazanov // Plasma Sci. Institute of Electrical and Electronics Engineers Inc. — 2019. — Vol. 47(8). — P. 4159–4164. DOI: 10.1109/TPS.2019.2927843

6 Ussenov Y.A. Particle formation during deposition of SiOx nanostructured thin films by atmospheric pressure plasma jet / Y.A. Ussenov, L. Hansen, T. Krueger, T.S. Ramazanov, H. Kersten // Jpn. J. Appl. Phys.– 2020. –Vol. 59(3). — P. 14–23. DOI: 10.35848/1347–4065/ab72ca

7 Xu X. Dielectric Barrier Discharge-Properties and Applications / X. Xu // Thin Solid Films. — 2001. — Vol. 390(1–2). — P. 237–242. DOI: 10.1016/S0040–6090(01)00956–7

8 Carbone E. Thomson scattering on non-equilibrium low density plasmas: Principles, practice and challenges / E. Carbone, S. Nijdam // Plasma Phys. Control. Fusion. IOP Publishing. — 2015. — Vol. 57(1). — P. 014–026. DOI: 1088/0741–3335/57/1/014026

9 Sretenovic' G.B. Thomson scattering on non-equilibrium low density plasmas: Principles, practice and challengesc / G.B. Sretenovic', I.B. Krstic', V.V. Kovac˘evic´, B.M. Obradovic´, M.M. Kuraica // Appl. Phys. Lett. — 2011. — Vol. 99(1). — P. 161502–1. DOI: 10.1063/1.3653474

10 Ramanujam N. Fluorescence spectroscopy of neoplastic and non-neoplastic tissues / N. Ramanujam // Neoplasia. Neoplasia Press, Inc. — 2000. — Vol. 2(1–2). — P. 89–117. DOI: 10.1038/sj.neo.7900077

11 Hagelaar G.J.M. Solving the Boltzmann equation to obtain electron transport coefficients and rate coefficients for fluid models / G.J.M. Hagelaar, L.C. Pitchford // Plasma Sources Sci. Technol. — 2005. — Vol. 14(4). — P. 722–733. DOI: 10.1088/0963–0252/14/4/011

12 Акильдинова А.К. Электрические и оптические свойства диэлектрического копланарного поверхностного разряда / А.К. Акильдинова, Е.А. Усенов, А.С. Пазыл, М.Т. Габдуллин, М.К. Досболаев, Т.С. Рамазанов, Т.Т. Данияров // Вестн. Казах. нац. ун-та. Сер. физ. — 2018. — № 2 (65). — С. 58–65.

13 Kozlov K.V. Spatio-temporally resolved spectroscopic diagnostics of the barrier discharge in air at atmospheric pressure / K.V. Kozlov, H-E. Wagner, R. Brandenburg, P.Michel // J. Phys. D. Appl. Phys. — 2001. — Vol. 34(21). — P. 3164–3176. DOI: 10.1088/0022–3727/34/21/309

14 Hagelaar G.J.M. Brief documentation of BOLSIG + version 03 [Electronic resource] / G.J.M. Hagelaar. — Access mode: http://www.bolsig.laplace.univ-tlse.fr/wp-content/uploads/2016/03/bolsigdoc0316.pdf– 2016.

15 Korbut A.N. Emission properties of an atmospheric-pressure helium plasma jet generated by a barrier discharge / A.N. Korbut, V.A. Kelman, Yu.V.Zhmenyak, M.S. Klenovskii // Opt. Spectrosc. — 2014. — Vol. 116(6). — P. 919–925. DOI: 10.1134/S0030400X14040146

16 Berlich R. Spatially resolved measurement of femtosecond laser induced refractive index changes in transparent materials / R.Berlich, J.Choi, C.Mazuir, W.V. Schoenfeld, S.Nolte, M. Richardson // Opt. Lett. — 2012. — Vol. 37(14). — P. 3003–3005. DOI: 10.1364/OL.37.003003

17 Starikovskaia S.M. On electric field measurements in surface dielectric barrier discharge / S.M. Starikovskaia, K. Allegraud, O. Guaitella, A. Rousseau // J. Phys. D. Appl. Phys. — 2010. — Vol. 43(12). — P. 124007–1. DOI: 10.1088/0022–3727/43/12/124007

18 Roupassov D.V. Flow separation control by plasma actuator with nanosecond pulsed-periodic discharge / D.V. Roupassov, A.A. Nikipelov, M.M. Nudnova, A.Yu. Starikovskii // AIAA J. — 2009. — Vol. 47(1). — P. 168–185. DOI: 10.2514/1.38113

19 Takahashi K. Electron energy distribution of a current-free double layer: Druyvesteyn theory and experiments / K. Takahashi, C. Charles, R.W. Boswell, T. Fujiwara // Phys. Rev. Lett. — 2011. — Vol. 107(3). — P. 1–4. DOI: 10.1103/PhysRevLett.107.035002

А.А. Муталип, Е.А. Усенов, А.К. Акильдинова,
М.Қ. Досболаев, М.Т. Габдуллин, Т.С. Рамазанов

Диэлектрлік беттік тосқауылдық разрядтағы плазманың меншікті электр өрісін анықтау

Мақалада атмосфералық қысымдағы диэлектрлік копланарлық беттік тосқауылдық разрядтағы (ДКБТР) меншікті электр өрісін (E/n) эксперименттік түрде анықтау көрсетілген. Плазма мен эксперименталдық қондырғының параметрлері сипатталған және плазманың оптикалық эмиссиялық спектрі алынды. Оптикалық эмиссиялық спектроскопияның нәтижелері ДКБТР сәулелену спектрінде молекулалық азот жолақтарының болуын көрсетті, атап айтқанда, екінші оң және бірінші теріс жүйелері, сонымен қатар интенсивтілігі төмен OH және NO спектрлік сызықтар жүйесі. Электрондардың негізгі тасымалдық қасиеттері ретінде қозғалғыштық, орташа энергия, диффузия коэффициенті BOLSIG+ ашық бағдарламалық жасақтамасын қолдана отырып есептелді. Меншікті электр өрісінің азоттың спектрлік сызықтарының интенсивтілігінің арақатынасына тәуелділігі, қуаттың және электрондар энергиясының таралу функциясының (ЭЭТФ) E/n-ге тәуелділігі

анықталды. BOLSIG+ бағдарламасында меншікті электр өрісін анықтау және спектрлік сызықтардың интенсивтілігін өлшеу алгоритмі блок-схема түрінде көрсетілген. Пайдаланылған әдіс оңайлығымен, қолжетімділігімен және әмбебаптығымен ерекшеленген.

Кілт сөздер: плазма, диэлектрлік барьерлік разряд, спектроскопия, меншікті электр өрісі, сызықтар интенсивтілігі, азот спектрі, Больцман теңдеуі.

А.А. Муталип, Е.А. Усенов, А.К. Акильдинова,
М.Қ. Досболаев, М.Т. Габдуллин, Т.С. Рамазанов

Определение приведенного электрического поля в плазме диэлектрического поверхностного барьерного разряда

В статье продемонстрировано экспериментальное определение приведенного электрического поля (E/n) диэлектрического копланарного поверхностного барьерного разряда (ДКПБР) при атмосферном давлении. Описаны характеристики плазмы и экспериментальной установки, был получен оптический эмиссионный спектр плазмы. Результаты оптико-эмиссионной спектроскопии показали наличие в спектре излучения ДКПБР молекулярных полос азота, а именно второй положительной и первой отрицательной систем, а также линии OH и NO с низкой интенсивностью. Были рассчитаны основные транспортные свойства электронов, такие как подвижность, средняя энергия, коэффициент диффузии, с помощью открытого программного пакета BOLSIG+. Были получены зависимости соотношения интенсивностей спектральных линий азота от приведенного электрического поля от мощности, функции распределения энергии электронов (ФРЭЭ) от приведенного электрического поля. Представлен алгоритм действий для определения приведенного электрического поля в программе BOLSIG+ и экспериментального измерения интенсивности спектральных линий в виде блок-схемы. Использованный метод отличался достаточной простотой, доступностью и универсальностью.

Ключевые слова: плазма, диэлектрический барьерный разряд, спектроскопия, приведенное электрическое поле, интенсивность линий, спектр азота, уравнение Больцмана.

References

1 Brandenburg, R. (2017). Dielectric barrier discharges: Progress on plasma sources and on the understanding of regimes and single filaments. *Plasma Sources Sci. Technol., 26(5),* P. 3001–1.

2 Akishev, Y.S., Aponin, G., Balakirev, A., Grushin, M., Karalnik, V., & Trushkin, N. (2011). Role of the volume and surface breakdown in a formation of microdischarges in a steady-state DBD. *Eur. Phys. J. D., 61(2),* 421–429.

3 Usenov, E.A., Akishev, Yu. S., Petryakov, A.V., Ramazanov, T.S., Gabdullin, M.T., & Ashirbek A. (2020). The Memory Effect of Microdischarges in the Barrier Discharge in Airflow. *Plasma Phys. Reports, 46(4),* 459–464.

4 Penkov, O., Khadem, M., Won Suk Lim & Dae-Eun Kim (2015). A review of recent applications of atmospheric pressure plasma jets for materials processing. *Journal of Coatings Technology and Research, 12(1),* 225–235.

5 Ussenov, Y.A., Pazyl, A.S., Dosbolayev, M.K., Gabdullin, M.T., Daniyarov, T.T., & Ramazanov, T.S. (2019). Dust Particle Synthesis by the Combined Plasma Source at Atmospheric Pressure. *Plasma Sci. Institute of Electrical and Electronics Engineers Inc.,* 47(8), 4159–4164.

6 Ussenov, Y.A., Hansen, L., Krueger, T., Ramazanov, T.S., & Kersten, H. (2020). Particle formation during deposition of SiOx nanostructured thin films by atmospheric pressure plasma jet. *Jpn. J. Appl. Phys.,* 59(3), 14–23.

7 Xu, X. (2001). Dielectric Barrier Discharge-Properties and Applications. *Thin Solid Films,* 390(1–2), 237–242.

8 CarboneE.&NijdamS. (2015). Thomson scattering on non-equilibrium low density plasmas: Principles, practice and challenges. *Plasma Phys. Control. Fusion. IOP Publishing,* 57(1), 014–026.

9 Sretenovic', G.B., Krstic', I.B., Kovac˘evic´, V.V., Obradovic, B.M. & Kuraica, M.M. (2011). Spectroscopic measurement of electric field in atmospheric-pressure plasma jet operating in bullet mode. *Appl. Phys. Lett.,* 99(1), 161502–1.

10 Ramanujam, N. (2000). Fluorescence spectroscopy of neoplastic and non-neoplastic tissues. *Neoplasia. Neoplasia Press, Inc.,* 2(1–2), 89–117.

11 Hagelaar, G.J.M. & Pitchford, L.C. (2005). Solving the Boltzmann equation to obtain electron transport coefficients and rate coefficients for fluid models. *Plasma Sources Sci. Technol.,* 14(4), 722–733.

12 Akildinova, A.K., Ussenov, Y.A., Pazyl, A.S., Gabdullin, M.T., Dosbolayev, M.K., Ramazanov, T.S., & Daniyarov, T.T. (2018). Electricheskie i opticheskie svoistva dielektricheskogo koplanarnogo poverkhnostnogo razriada [Electrical and optical properties of diffuse coplanar surface barrier discharge]. *Vestnik Kazakhskoho natsionalnogo universiteta. Seriia fizicheskaia, 2(65),* 58–65 [in Russian].

13 Kozlov, K.V., Wagner, H-E., Brandenburg, R. & Michel, P. (2001). Spatio-temporally resolved spectroscopic diagnostics of the barrier discharge in air at atmospheric pressure. *J. Phys. D. Appl. Phys.,* 34(21), 3164–3176.

14 Hagelaar, G.J.M. (2016). Brief documentation of BOLSIG + version 03. *bolsig.laplace.univ-tlse.fr*. Retrived from http://www.bolsig.laplace.univ-tlse.fr/wp-content/uploads/2016/03/bolsigdoc0316.pdf

15 Korbut, A.N., Kelman, V.A.,.Zhmenyak, Yu.V., & Klenovskii, M.S. (2014). Emission properties of an atmospheric-pressure helium plasma jet generated by a barrier discharge. *Opt. Spectrosc.,* 116(6), 919–925.

16 Berlich, R., Choi, J., Mazuir, C., Schoenfeld, W.V., Nolte, S., & Richardson, M. (2012). Spatially resolved measurement of femtosecond laser induced refractive index changes in transparent materials. *Opt. Lett.,* 37(14), 3003–3005.

17 Starikovskaia, S.M., Allegraud, K., Guaitella, O. & Rousseau, A. (2010). On electric field measurements in surface dielectric barrier discharge. *J. Phys. D. Appl. Phys.,*43(12), 124007–1.

18 Roupassov, D.V., NikipelovA.A., Nudnova, M.M. &Starikovskii, A.Yu. (2009). Flow separation control by plasma actuator with nanosecond pulsed-periodic discharge. *AIAA J.,* 47(1), 168–185.

19 Takahashi, K., Charles, C., Boswell, R.W. & Fujiwara, T. (2011). Electron energy distribution of a current-free double layer: Druyvesteyn theory and experiments. *Phys. Rev. Lett.,* 107(3), 1–4.